Chlorination-Methylation of the Hydrogen-terminated Silicon (111) Surface Can Induce a Stacking Fault in the Presence of Etch Pits

Santiago D. Solares, Hongbin Yu, Lauren J. Webb, Nathan S. Lewis, James R. Heath,**

*and William A. Goddard III**

Division of Chemistry and Chemical Engineering, California Institute of Technology, Pasadena, California, 91125

*Corresponding authors: wag@wag.caltech.edu, nslewis@caltech.edu, heath@caltech.edu

Supporting Information

1. Computational Methods

Periodic DFT calculations were conducted using two software packages:

(1) SeqQuest (Sandia National Labs, Albuquerque, NM)[1], a general-purpose electronic structure code for periodic and non-periodic systems, with norm-conserving pseudopotentials and optimized contracted *Gaussian* basis sets. SeqQuest calculations were performed using the PBE[2] flavor of DFT with a valence double-zeta basis set plus polarization functions (denoted vDZp) with pseudopotential for silicon and carbon, while for hydrogen both double-zeta and triple-zeta basis sets (6311G basis set) plus polarization functions (denoted vDZp and vTZp, respectively) with and without pseudopotential were used.

(2) Castep21 (Accelrys, San Diego CA), a general-purpose electronic code for 3D periodic structures, which uses ultra-soft pseudopotentials and *plane wave* basis sets. Here we also used the PBE[2] approximation with a plane wave kinetic energy cutoff of 380 eV and with pseudopotentials for all atoms.

For the PBC calculations 8 k-points were used for each horizontal unit cell vector of the 1x1 Si(111) unit cell. The number of k-points for all other structures was adjusted inversely proportional to unit cell dimensions.

All non-periodic DFT calculations were performed using Jaguar 5.5 software (Schrödinger, Portland, OR). For the molecules described in section 1.3 the B3LYP flavor of DFT was used with both Gaussian triple-zeta (6311G**++) and Dunning triple-zeta (cc-PVTZ++) basis sets. The change in free energy for the Grignard reaction [Si(111)-Cl + CH_3-Mg-Cl → Si(111)-CH_3 + $MgCl_2$] in THF solvent (ΔG^{298° = -41.0 kcal/mol) was also estimated using non-periodic DFT at the B3LYP level of theory, but with 631G** basis sets and using the Poisson-Boltzmann continuum solvation model. For this calculation, the Si(111) sites were modeled as Si_4H_9 clusters to which Cl or CH_3 were bonded.

For the MD simulations (see section 1.4.1), Cerius2 software (Accelrys, San Diego, CA) was used with previously reported force field parameters for silicon[3] and hydrocarbons[4], with the H-C-Si-Si torsional force field parameter adjusted to 2.945 kcal/mol to match the DFT (SeqQuest) calculations on the Si(111)-CH_3 model described in 1.1.1, using vDZp basis sets and pseudopotentials for all atoms. Atomic charges for the MD simulations were computed using the Charge Equilibration method. [5]

All surface unit cell dimensions were based on the calculated PBE equilibrium value of the Si crystal lattice, equal to 5.431 Å.

1.1 Periodic DFT Geometry Optimization of 1x1 Unit Cells

To calculate the optimum torsion angle for various systems resembling our experimental surfaces, the geometry was optimized through minimizing the total energy for the following cases:

1.1.1 Case 1 - Si(111)-CH_3 surface using Gaussian basis functions (SeqQuest): The Si(111)-CH_3 1x1 unit cell was modeled using a 2D slab with eight bulk silicon layers, terminated by hydrogen on the bottom surface

(Si-H bond perpendicular to the surface). The unit cell thus has 13 atoms. Considering the surface to be perpendicular to the z-axis, the lateral unit cell parameters were kept fixed at the crystal value of 3.86 Å. The bottom surface hydrogen atom was kept fixed during the calculations while all the silicon atoms and the methyl group were allowed to relax. All calculations were performed using the vDZp basis set and pseudopotentials for silicon and carbon. For hydrogen various cases were considered with vDZp and vTZp basis sets (6311G), with and without pseudopotential.

1.1.2 Case 2 - Si(111)-CH_3 surface using plane wave basis functions (Castep21): The same Si(111)-CH_3 1x1 unit cell was modeled as in case 1, but using a 3D structure, consisting of a 2D surface slab with 20 Å of vacuum above the surface.

1.1.3 Case 3 – Si(111), Si(111)-H, Si(111)-Cl, and Si(111)-CH_3 surfaces with a stacking fault using Gaussian functions (SeqQuest): A Si(111) unit cell similar to that of case 1 (without functionalization or functionalized with H, Cl and CH_3) was modeled, but a stacking fault was introduced between the 1st and 2nd layers. We also calculated the bulk stacking fault energy using a 12-layer 3D periodic bulk model of the silicon *crystal*.

1.2 Periodic DFT calculation of Strain Energy at the Step Edges

To determine whether binding of chemisorbed species to systems containing etch pits might affect the relative energies for stacking faults, periodic Si(111)-H, Si(111)-Cl and Si(111)-CH_3 unit cells were constructed containing 10 bulk Si layers and a partial double layer of either the $<1\bar{1}2>$ (observed in our experiments) or $<\bar{1}\bar{1}2>$ step edge termination (see Figure S-1). [Note that the $<\bar{1}\bar{1}2>$ step reconstructs to have the substituents perpendicular to the edge surface and to lower its energy (see section 4). [6,7]]. For both step edges, the bond energy of each substituent (H, Cl or CH_3) to the edge site was then computed by removing one of the substituents and substracting this bond energy from the bond energy on a perfect surface, to obtain the strain energy at the edge site. Calculations were also performed on non-functionalized Si structures (see Figure S-2) to obtain the contribution to the surface energy due to the presence of a step edge in a bare 1x1 Si(111) surface.

All structures were 1 cell deep, except the *unreconstructed* $<\bar{1}\bar{1}2>$ structure, which was 4 unit cells deep, to allow the formation of dimers between adjacent edge atoms containing two dangling bonds each. The structure of the Si(111)-CH_3 did not change when the cell depth was increased up to 4 unit cells deep.

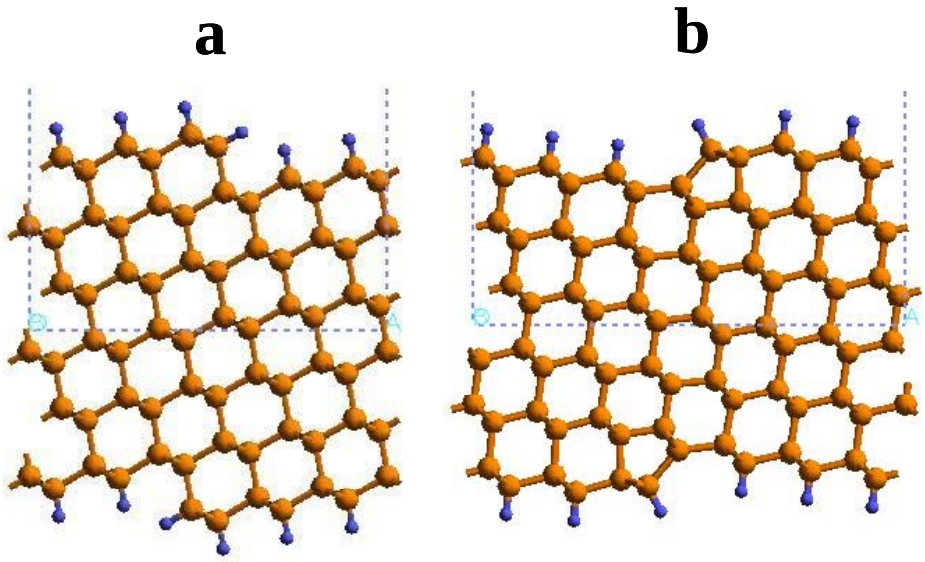

Figure S-1. Side view of the Si(111)-H periodic unit cells used for the calculation of the strain energy difference between the $<11\bar{2}>$ (a) and $<\bar{1}\bar{1}2>$ (b) step edge terminations. The $<11\bar{2}>$ unit cell (a) was obtained by cutting the Si crystal along the $<664>$ plane, and the $<\bar{1}\bar{1}2>$ unit cell (b) was obtained by cutting the crystal along the $<668>$ plane. Similar models were constructed for Si(111), Si(111)-Cl and Si(111)-CH_3.

1.3 Non-periodic DFT Geometry Optimization

To determine the trends in the torsion angles of small systems containing tetrahedral silicon and carbon atoms, the geometry for several molecules was optimized using the triple-zeta 6311G**++ and cc-PVTZ++ basis sets at the B3LYP theory level. This process was performed for fixed torsion angles of 0° (eclipsed) and 60° (staggered) for the CH_3 or SiH_3 groups, as appropriate (see Table S-1), and without any constraints (to

calculate the equilibrium torsion angle). The torsional energy barriers were calculated from the difference in total energy between the eclipsed and staggered configurations for the following molecules:

i. *Pure hydrocarbons:* $H_3C\text{-}CH_3$ and $H_3C\text{-}C\text{-}(CH_3)_3$

ii. *Pure silanes:* $H_3Si\text{-}SiH_3$ and $H_3Si\text{-}Si\text{-}(SiH_3)_3$

iii. *Molecules containing silicon, carbon and hydrogen:* $H_3C\text{-}SiH_3$ and $H_3C\text{-}Si\text{-}(SiH_3)_3$ (this molecule resembles the structure of the $Si(111)\text{-}CH_3$ surface most closely)

1.4 Molecular Dynamics Calculations

1.4.1 Role of Methyl-Methyl Interactions

To evaluate the relative importance of the methyl-methyl interactions in determining the H-C-Si-Si torsion angle, the slab geometry was optimized for the periodic $Si(111)\text{-}CH_3$ model described in 1.1.1, but with the C-Si bond length artificially extended to 1 nm (equilibrium bond length is 0.18 nm) and with the H-C-Si-Si torsional barrier set to 0 kcal/mol. This determined the optimum torsion angle preferred by the interactions between the methyl groups, while eschewing any surface effects due to the silicon atoms (calculated to be 30°). Note that this calculation cannot be performed with QM because the artificial lengthening of the Si-C bond causes the remaining CH_3 groups to behave as CH_3 radicals, which are planar and reactive.

2. Torsional Barriers of Small Organic Molecules

Table S-1 contains the calculated torsional barriers for small organic molecules containing carbon, silicon and hydrogen at the B3LYP level of theory [calculations at the HF and Becke 3 (GGA II / PW91) levels were also performed and gave similar results (not shown)]. The lowest energy configuration is *staggered* in all cases, corresponding to a torsion angle of 60° (The torsion angle of interest is indicated in the first column of the table).

*Table S-1: Torsional energy barrier for various small molecules at the DFT B3LYP level of QM using the CC-PVTZ++ (and 6311G**++) basis sets. The most stable configuration is staggered for all molecules.*

Molecule	Torsion angle of interest	DFT Torsional barrier, kcal/mol
Pure hydrocarbons		
H_3C-CH_3	H-C-C-H	2.61 (2.70)
H_3C-C-$(CH_3)_3$	H-C-C-C	3.62 (3.63)
Pure silanes		
H_3Si-SiH_3	H-Si-Si-H	0.96 (0.93)
H_3Si-Si-$(SiH_3)_3$	H-Si-Si-Si	0.76 (0.80)
Molecules containing Si, C and H		
H_3C-SiH_3	H-C-Si-H	1.45 (1.41)
H_3C-Si-$(SiH_3)_3$	H-C-Si-Si	1.48 (1.47)

3. Periodic DFT Equilibrium Geometry of Si(111)-CH_3

The calculated H-C-Si-Si torsion angle for periodic DFT calculations (using both Gaussian and plane wave basis sets) is shown in Table S-2. We believe that the most accurate results are for case 1 with the vTZp basis and without pseudopotential (in boldface), leading to a torsion angle of 37.5º. This shows that the interactions between H atoms of adjacent methyls dominate (preferring 30º) but are distorted by 7.5º toward the *staggered* configuration (60º). Comparison of case 3 to case 1 shows that introduction of a stacking fault between the 1st and 2nd Si layers does *not* change the torsion angle with respect to the *second* Si layer. The Si-C bond and the H-C-H angle are also listed in Table S-2. All values are close to those calculated for the H_3C-Si-$(SiH_3)_3$ cluster (1.91 Å and 108.0º respectively).

Table S-2: Si(111)-CH_3 equilibrium surface geometry from periodic DFT calculations for various basis sets, hydrogen pseudopotentials and silicon crystal stackings. Standard basis sets (Gaussian or plane waves, as

appropriate) and pseudopotentials were used for silicon and carbon in all cases. We consider the triple zeta calculation with no H pseudopotential (in boldface) as the most accurate method.

Basis set used for hydrogen atoms	H-C-Si-Si torsion angle, degrees	Si-C bond length, Angstroms	H-C-H bond angle, degrees
vDZp with H pseudopotential (case 1)	36.2	1.94	107.6
vTZp with H pseudopotential (case 1)	36.2	1.93	106.4
vDZp with no H pseudopotential (case 1)	38.2	1.94	107.8
vTZp with no H pseudopotential (case 1)	**37.5**	**1.93**	**107.7**
Plane waves with pseudopotential (case 2)	38.7	1.89	108.0
vDZp with H pseudopotential and a stacking fault between the 1st and 2nd Si layers (case 3)	36.7	1.93	107.9

4. Strain and Geometry of $<1\bar{1}2>$ and $<\bar{1}\bar{1}2>$ Step Edges

Table S-3 contains the calculated strain energy for both types of step edges and the difference between them for each of the substituents (H, Cl or CH_3). These results show that the strain energy difference is small for Si(111)-H but not for Si(111)-Cl or Si(111)-CH_3, both of which exhibit a strong preference for the reconstructed $<\bar{1}\bar{1}2>$ structure. Table S-4 provides the surface energy contribution of the step edges in a 1x1 Si(111) surface containing a single infinitely long step [This energy includes one dangling bond on the $<1\bar{1}2>$ edge, one dangling bond on the *unreconstructed* $<\bar{1}\bar{1}2>$ edge (the second dangling bond is paired up with a dangling bond on the adjacent edge site), and no dangling bonds on the *reconstructed* $<\bar{1}\bar{1}2>$ edge (the reconstruction eliminates the dangling bonds on the edge as shown in Figure S-2)]. Although the *reconstructed* $<\bar{1}\bar{1}2>$ structure has greater strain in the bonds and angles, it has the lowest energy of all due to the elimination of the edge dangling bond. The second lowest energy corresponds to the $<1\bar{1}2>$ edge, and the highest energy to the *unreconstructed* $<\bar{1}\bar{1}2>$ structure.

Table S-3: Calculated strain energy (eV per site) at the step edges.

	$<11\bar{2}>$	$<\bar{1}\bar{1}2>$	**Difference** $<11\bar{2}> - <\bar{1}\bar{1}2>$
Si(111)-H	-0.01	-0.06	0.05
Si(111)-Cl	0.57	-0.01	0.58
Si(111)-CH_3	0.60	-0.07	0.67

Table S-4: Calculated surface energy contribution due to the presence of a step edge in the bare 1x1 Si(111) surface. The different structures are illustrated in Figure S-2.

Step edge	**Edge dangling bonds**	**Energy, eV/site**
$<11\bar{2}>$	1	1.35
$<\bar{1}\bar{1}2>$ unreconstructed[a]	1	1.60
$<\bar{1}\bar{1}2>$ reconstructed[b]	0	0.79

[a]In this structure, the edge atoms in adjacent positions form dimers to avoid having two dangling bonds each

[b]The reconstruction eliminates the edge dangling bonds (see Figure S-2)

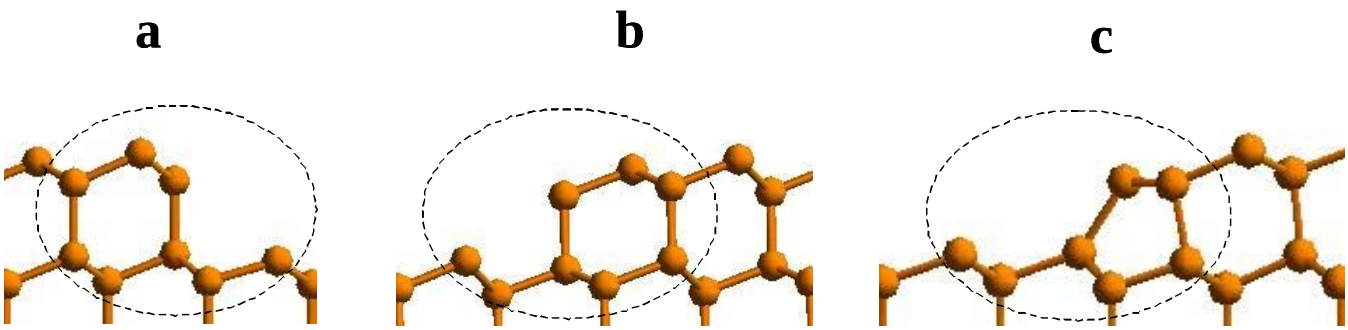

Figure S-2. Structures of the Si(111) surface step edges: (a) $<11\bar{2}>$ edge, (b) *unreconstructed* $<\bar{1}\bar{1}2>$ edge, and (c) *reconstructed* $<\bar{1}\bar{1}2>$ edge.

The most relevant geometry parameters calculated for the $<1\bar{1}2>$ and for the *reconstructed* $<\bar{1}\bar{1}2>$ step edge structures described in section 1. 2 are illustrated in Figure S-3 and are summarized in Tables S-5 and S-6 [we did not calculate these parameters for the *unreconstructed* $<\bar{1}\bar{1}2>$ structure since, according to Table S-4, it has the highest energy, and since its substituents are not perpendicular to the edge surface, which leads to additional strain due to nearest neighbor steric interactions]. In general, the $<1\bar{1}2>$ edge has smaller nearest neighbor distances (leading to greater steric repulsions), and has bonds and angles that are closer to those in the bulk crystal (leading to lower bond and angle strain).

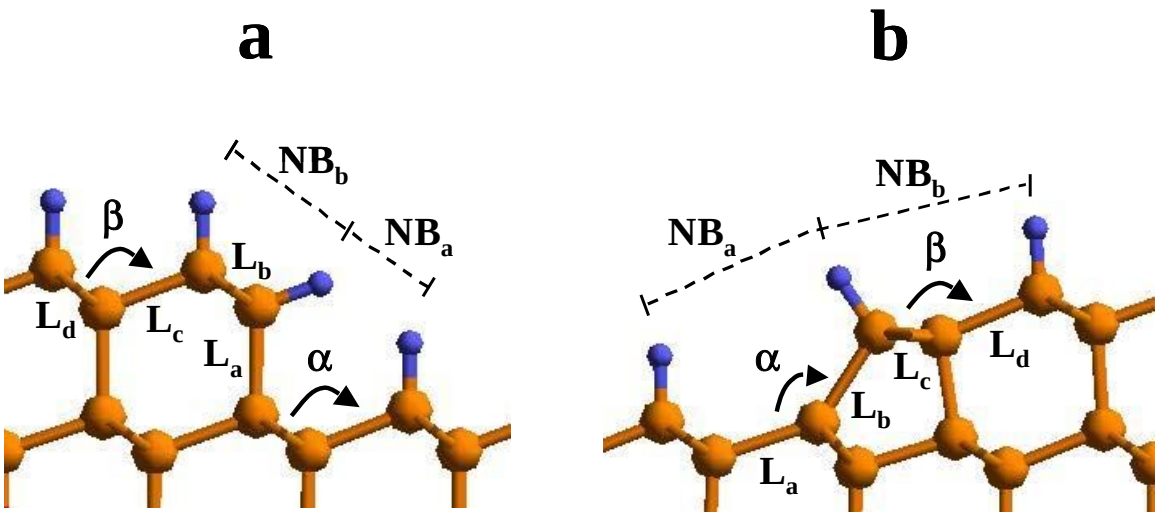

Figure S-3. Relevant geometry parameters of the step edge terminations for Si(111), Si(111)-H, Si(111)-Cl and Si(111)-CH_3 surfaces. (a) $<1\bar{1}2>$, and (b) reconstructed $<\bar{1}\bar{1}2>$. L_a, L_b, L_c and L_d represent Si-Si bond lengths, while α and β represent Si-Si-Si bond angles. Their values are summarized in Table S-5. The nonbond distances relevant for understanding the relative strain energies are denoted NB_a and NB_b and their values are summarized in Table S-6.

Table S-5: Calculated geometry parameters for the $<11\bar{2}>$ and $<\bar{1}\bar{1}2>$ step edge terminations for Si(111), Si(111)-H, Si(111)-Cl and Si(111)-CH_3 surfaces, as defined in Figure S-3. All distances and angles are given in Å and degrees respectively (for comparison, the experimental bulk Si-Si bond length and bond angle are 2.36 Å and 109.41° respectively)

Surface	L_a	L_b	L_c	L_d	α	β
$<11\bar{2}>$						
Si(111)	2.37	2.33	2.37	2.34	109.4	110.8
Si(111)-H	2.37	2.36	2.36	2.35	108.7	110.2
Si(111)-Cl	2.42	2.35	2.37	2.34	110.8	108.8
Si(111)-CH_3	2.41	2.35	2.32	2.35	108.7	106.9
$<\bar{1}\bar{1}2>$						
Si(111)	2.42	2.47	2.38	2.39	134.9	122.3
Si(111)-H	2.42	2.48	2.39	2.39	136.4	121.3
Si(111)-Cl	2.41	2.47	2.39	2.39	137.5	122.3
Si(111)-CH_3	2.43	2.47	2.39	2.41	136.0	121.4

Table S-6: Calculated nearest neighbor distances (Å) for substituents on $<11\bar{2}>$ and $<\bar{1}\bar{1}2>$ step edges for Si(111)-H, Si(111)-Cl and Si(111)-CH_3 surfaces. In each case, the distance is provided with respect to a neighbor on the step edge, on the pit (NB_a) or on the terrace (NB_b) [See Figure S-3 for notation]. For CH_3, the distances correspond to the smallest H-H distance between adjacent groups.

	$<11\bar{2}>$			$<\bar{1}\bar{1}2>$		
Surface	Edge-edge	NB_a	NB_b	Edge-edge	NB_a	NB_b
Si(111)-H	3.84	2.97	3.61	3.84	4.79	4.91
Si(111)-Cl	3.84	3.23	4.10	3.84	4.29	5.29
Si(111)-CH_3	2.43	2.07	2.52	2.29	2.48	3.89

An important observation in the Si(111)-Cl surface containing the $<11\bar{2}>$ step is the presence of overstretched Si-Si bonds (Figure S-4), caused by the Cl---Cl nearest neighbor repulsions. This is a manifestation of the high surface strain present at the edge and suggests that surface reconstruction processes are likely to occur. We did not observe this for Si(111)-CH_3, although the DFT calculations indicate that this surface has greater edge strain than Si(111)-Cl.

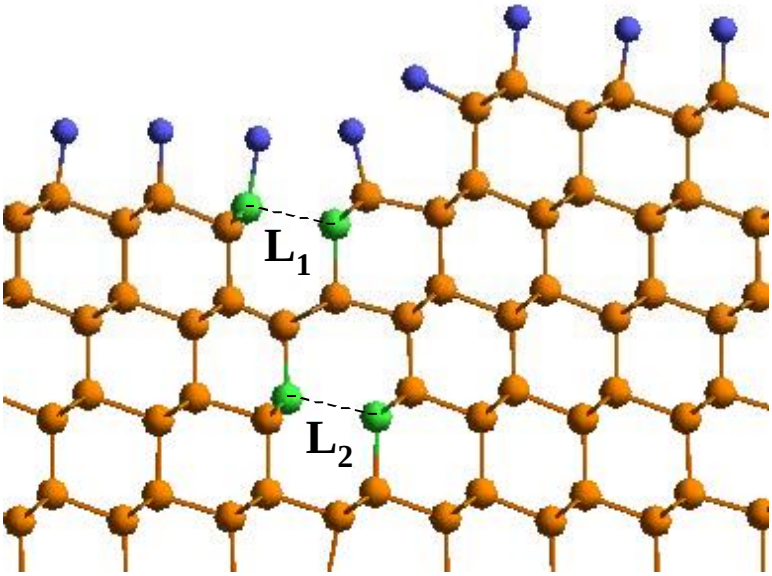

Figure S-4. Illustration of overstretched Si-Si bonds in the chlorinated $<11\bar{2}>$ step edge. The blue atoms are Cl, the orange atoms are bulk Si and the green atoms are Si with overstretched bonds. In the optimum structure, L_1 = 2.82 Å and L_2 = 2.87 Å (compare to L_{bulk} = 2.36 Å)

5. Expanded Version of the Stacking Fault Discussion in the Main Paper

Since a single stacking fault between the 1st and 2nd Si layers would have the effect of rotating the apparent torsion of the CH_3 by 60° with respect to the bulk (below the 2nd Si layer), we carried out DFT calculations on Si(111)-H, Si(111)-Cl and Si(111)-CH_3 surface slabs containing a stacking fault between the 1st and 2nd Si layers. These calculations showed that the stacking fault did *not* change the H-C-Si-Si torsion angle, but that the *apparent* torsion angle with respect to the bulk changed from 37° to 23°, thus providing a possible

explanation for the observed discrepancy between the theoretical and experimental results. However the DFT results showed that a stacking fault is *not* favored for any of these perfect surfaces, as indicated in the first column of Table 1 of the paper (Table S-7 below), which shows the stacking fault energy cost per site for perfect Si(111)-H, Si(111)-Cl and Si(111)-CH_3 surfaces. Since no other geometrical explanation can reconcile the experimental and theoretical results we then considered how a stacking fault could be stabilized.

Since ~16% of the area on our Si(111)-CH_3 surface was covered by etch pits, we considered whether chemisorbed species on the step edges might stabilize the stacking fault on the terrace. To test this possibility, periodic DFT calculations were performed on Si(111)-H, Si(111)-Cl and Si(111)-CH_3 models containing an infinite $<1\bar{1}2>$ or $<\bar{1}\bar{1}2>$ step edge [the two step edge structures are shown in Figure S-5 (Figure 2 of the paper)]. [6] We then calculated the difference in strain between these two step edges, per edge site. The strain energy difference was found to be small for Si(111)-H, but not for Si(111)-Cl and Si(111)-CH_3, which exhibit a *strong* preference for $<\bar{1}\bar{1}2>$. The second column of Table S-7 contains the strain energy difference between the two step edge structures and indicates that this difference is ~11.6 and ~13.4 times larger for Si(111)-Cl and Si(111)-CH_3, respectively, than for Si(111)-H.

Table S-7. Stacking fault energy cost per surface site of perfect surfaces, differential strain energy per edge site ($<1\bar{1}2>$ - $<\bar{1}\bar{1}2>$ *step edge terminations) and equivalent faulted sites per edge site differential strain.*[a]

Surface	**$\Delta E_{stacking\ fault}$**[b] **eV/1x1 cell**	**δE_{strain} eV/edge site**	**Equivalent faulted/edge sites** [a]
Si(111)	0.048	N/A	N/A
Si(111)-H	0.031	0.05	1
Si(111)-Cl	0.033	0.58	17
Si(111)-CH_3	0.034	0.67	19

[a] This quantity was obtained by dividing numbers in the 2nd column by those in the 1st column and meaningful only if $\delta E_{strain} > 0$ (i.e. when the stacking fault is favorable).
[b]The calculated *bulk* Si value of $\Delta E_{stacking\ fault}$ is 0.015 eV/1x1 cell

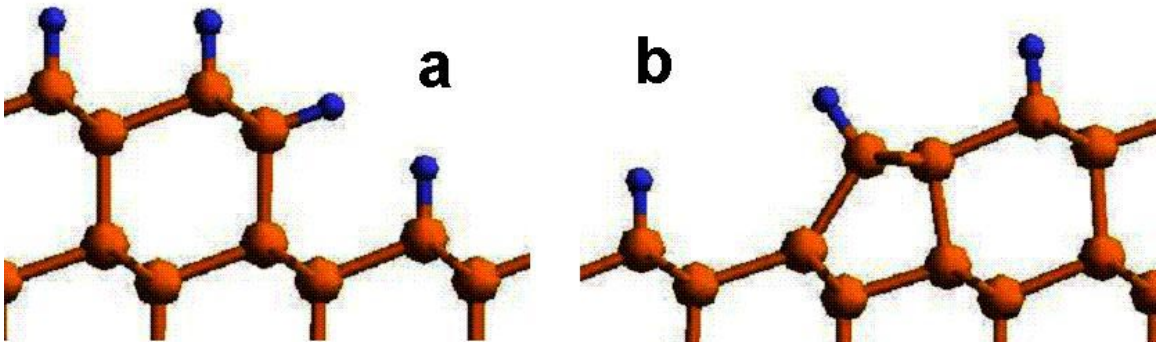

Figure S-5. $<1\bar{1}2>$ (a) and $<\bar{1}\bar{1}2>$ (b) step edges for the Si(111)-H surface. Note that the $<\bar{1}\bar{1}2>$ structure (b) has reconstructed in order to have its substituents perpendicular to the edge surface and to lower its energy. [6]

To understand these differences, consider first Si(111)-H and the spacing of the H atoms on the two step edges shown in Figure S-5. On this surface the Si-Si bond lengths and Si-Si-Si bond angles are close to the bulk value for the structure containing the $<1\bar{1}2>$ step edge, (See Figure S-3 and Tables S-5 and S-6), and all H---H nearest neighbors distances are greater than 2.97 Å causing no significant unfavorable interactions between the small H atoms (compare to the shortest H---H distance in polyethylene, 2.51 Å). In contrast, for Si(111)-Cl, some of the nearest neighbor Cl---Cl distances are as low as 3.23 Å for the structure containing the $<1\bar{1}2>$ step edge, but they are always greater than 3.84 Å for the structure containing the $<\bar{1}\bar{1}2>$ step edge. Since the van der Waals radius of the Cl atom is ~3.95 Å,[4] substantial steric repulsions are expected for the $<1\bar{1}2>$ step edge termination. Indeed the QM calculations indicate that Si-Cl bond on the $<\bar{1}\bar{1}2>$ step edge is 0.58 eV stronger than on the $<1\bar{1}2>$ step edge (See Table S-7, 2nd column). For Si(111)-CH_3, the nearest neighbor H---H distance on the $<1\bar{1}2>$ step edge is 2.07 Å (0.44 Å shorter than in polyethylene!), whereas the shortest distance on $<\bar{1}\bar{1}2>$ is 2.29 Å, resulting in a Si-CH_3 bond with significantly lower strain energy on $<\bar{1}\bar{1}2>$ than on $<1\bar{1}2>$ (by 0.67 eV).

The samples in the 4 K STM experiments used the Si(111)-H surface as an intermediate step in preparing the methylated surface. The step edges around the etch pits were verified to be in the $<1\bar{1}2>$ family, and their

orientation did not change during the subsequent chlorination and alkylation steps (using PCl_5 and CH_3MgCl in THF solvent).[8] Hence, relief of the strain for Si(111)-Cl and Si(111)-CH_3 through the formation of the more favorable step edge termination shown in Fig. 2b, requires the introduction of a stacking fault between the 1st and 2nd Si layers *on the terraces* [note that when the step edge orientation is $<11\bar{2}>$, the *normal* crystal has the structure shown in Figure S-5a, while the *faulted* crystal has the structure in Figure S-5b]. Taking the difference in strain energy between the two types of step edges as the driving force for the formation of the stacking fault, and dividing this by the stacking fault energy cost, yields the number of equivalent faulted sites (given in the 3rd column of Table S-7) that this strain energy is able to induce (neglecting the energy of the rows of Si dimers at the borders between faulted and unfaulted regions[6]). Thus, allowing one edge site to transform from the structure of Figure S-5a to that of Figure S-5b would compensate for ~17 *faulted* sites on Si(111)-Cl, and for ~19 *faulted* sites on Si(111)-CH_3. This ratio is greater than the ratio of terrace to edge sites on the experimental Si(111)-CH_3 surface (~13), indicating that a full stacking fault on the terraces is energetically possible.

The theory-derived conclusion that there is a stacking fault in the Si(111)-CH_3 surface is consistent with the STM experiments of Ithckawitz et al,[6] who observed stacking faults on terrace regions adjacent to $<11\bar{2}>$ steps on Si(111)-Cl. They did *not* observe full stacking faults, but with their method [exposure of a DAS 7x7 Si(111) surface to Cl_2 gas at 673 – 773 K], the DAS (7x7) → (1x1) surface reconstruction occurs predominantly along step edges. [6] In some cases they may have also examined the surface structure before it transformed fully into a 1x1 Si(111)-Cl [the authors explain in their publication that it is not necessary that the halogenation reaction runs to completion in order to observe the stacking faults on the step edges. [6]]. Since the CH_3MgCl Grignard reagent used in our experiments is appreciably larger than Cl_2, it is plausible that steric interactions would play an even more significant role in the formation of a stacking fault in our Si(111)-CH_3 samples than on their halogenated samples.

The Si(111)-CH_3 surfaces were prepared at THF reflux temperature (~65°), at which Si(111) surface reconstructions do *not* occur spontaneously, but we believe they could be induced to accommodate the sterically hindered transition states expected for the Grignard conversion of the surface Cl to CH_3. This process is very

exothermic (DFT leads to ΔG^{298° = -41.0 kcal/mol, after including solvation using the Poisson-Boltzmann continuum model with a solvent dielectric constant of 7.6 for THF), so that the local temperature may increase the mobility of the atoms on the surface.

The emergence of a stacking fault during the chlorination-alkylation of Si(111)-H to produce Si(111)-CH_3 would resolve the discrepancy between theory and experiment. Thus the experimental torsion angle of 23° with respect to the bulk crystal would correspond to 37° with respect to the second Si layer on the terraces. On the other hand, the calculations find that the CH_3 groups in the etch pits have the normal torsion angle of 37.5° with respect to the bulk. Measuring this would provide an excellent validation of the new model, but current low temperature STM experiments can only observe the top layer. [8]

6. References

1. Schultz, P.A. Sandia National Labs., Albuquerque NM, SeqQuest Electronic Structure Code, http://dft.sandia.gov/Quest/

2. Perdew, J.P.; Burke, K.; Ernzerhof, M. *Phys. Rev. Lett.* **1996,** *77,* 3865.

3. Shapiro, I.R.; Solares, S.D.; Esplandiu, M.J.; Wade, L.A.; Goddard, W.A.; Collier, C.P. *J. Phys. Chem. B* **2004,** *108,* 13613.

4. Mayo, S.; Olafson, B. and Goddard, W. A. III. *J. Phys. Chem*. **1990**, 94, 8897.

5. Rappé, A.K. and Goddard, W.A. III. *J. Phys. Chem.* **1991,** *95,* 3358.

6. Itchkawitz, B.S.; McEllistrem, M.T.; Boland, J. *Phys. Rev. Lett.* **1997,** *78,* 98.

7. Redondo, A.; Goddard, W.A. III.; McGill, T.C. *Phys. Rev. B* **1981,** *24,* 6135.

8. Yu, H.; Webb, L.J.; Ries, R.S.; Solares, S.D.; Goddard, W.A. III; Heath, J.R.; Lewis, N.S. *J. Phys. Chem. B* **2005,** *109,* 671-674.